The Microwave Drill

E. Jerby,* V. Dikhtyar, O. Aktushev, U. Grosglick

We present a drilling method that is based on the phenomenon of local hot spot generation by near-field microwave radiation. The microwave drill is implemented by a coaxial near-field radiator fed by a conventional microwave source. The near-field radiator induces the microwave energy into a small volume in the drilled material under its surface, and a hot spot evolves in a rapid thermal-runaway process. The center electrode of the coaxial radiator itself is then inserted into the softened material to form the hole. The method is applicable for drilling a variety of nonconductive materials. It does not require fast rotating parts, and its operation makes no dust or noise.

Drilling holes is a fundamental operation in industrial, constructional, and geological works (*1*). Mechanical drills satisfy many of these needs, but their operation produces noise, vibrations, and dust effusion. Advanced drilling methods based on thermal and ablation effects make use of lasers (*2*), plasma jets, flames, and electrical heaters. Other methods employ ultrasonic devices, water jets, hydraulic presses, electron beams, and electro-erosion tools. Microwaves were proposed for destructive applications such as crushing of stones, mining, and concrete demolishing (*3*, *4*). Here we introduce a drilling method based on the effect of localized microwave heating.

Microwave energy is commonly used in a variety of industrial, scientific, and medical applications (*3*, *5*) for processing, drying, and heating. However, substantial problems can be caused by the thermal-runaway effect (*5*–*7*), in which the microwave heating results in a rapid nonuniform increase of the local temperature, thus creating a harmful hot spot. This effect, undesired in most applications, is used in the present study purposefully for the drilling operation.

The concentration of the microwave energy into a small hot spot (much smaller than the microwave wavelength) is the key principle underlying the microwave-drill invention (*8*). The near-field microwave radiator, illustrated in Fig. 1, is constructed as a coaxial waveguide ended with an extendable monopole antenna, which functions also as the drill bit. Initially, the microwave-energy deposition rate is highest at the material near the antenna. The subsurface tends to increase to a slightly higher temperature than the spontaneously cooled surface. Hence, the hottest zone becomes localized underneath the surface. Because hotter material usually absorbs microwaves better, the energy absorption in the subsurface is further increased. A hot spot is created, and the material becomes soft or molten. The coaxial center electrode is then inserted into this molten hot spot and shapes its boundaries. Finally, the electrode is removed from the hole, while the material cools down in its new shape.

The experimental setup consists of a power-adjustable microwave source (2.45-GHz, 1-kW magnetron), a directional coupler, and an impedance-matching tuner, in a cascade with the microwave-drill head. The latter is made as a rectangular-to-coaxial waveguide transition, as shown in Fig. 1. The coaxial center electrode is free to move as a drilling bit toward the drilled material. This electrode is usually made of a tungsten rod, and it sustains insertions into materials with melting temperatures up to 1500°C.

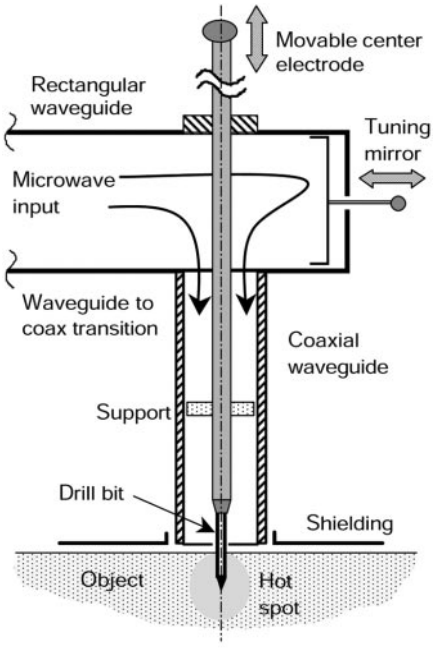

Fig. 1. Scheme illustrating the principle underlying the operation of a microwave drill, including a transition from a rectangular to a coaxial waveguide, a tuning mirror, and a movable center electrode. The electrode functions as both a monopole antenna and a drilling bit. The hot spot generated by the near-field microwaves softens the material and enables the drilling bit penetration into it.

For higher temperatures the tungsten rod is covered with an alumina tube or replaced by a silicon-carbide tip. The coaxial structure is cooled by a pressurized air flow, and thus it can support a 1-kW power transmission at a high standing-wave ratio.

During this study, microwave drills were successfully inserted into a variety of materials, including ceramics, concrete, basalt, glass, and silicon. In concrete, for example, 2-mm-diameter, 2-cm-deep holes were drilled within less than a minute each. Their cylindrical shape accuracy is comparable to that produced by mechanical drills. Holes of 1-mm diameter were made easily in ceramic and glass plates. Figure 2A shows the hot spot created inside a glass plate during the microwave drilling process (observed through the applicator side window). Figure 2B presents an example of a microwave-drilled hole in a low-purity alumina plate. The 6-mm hole diameter and 13-mm depth were generated after 2 min of 0.9-kW microwave illumination. For Fig. 2B, the molten material was deliberately left on the bore perimeter, for illustration, but would ordinarily be mechanically removed during or shortly after the drilling.

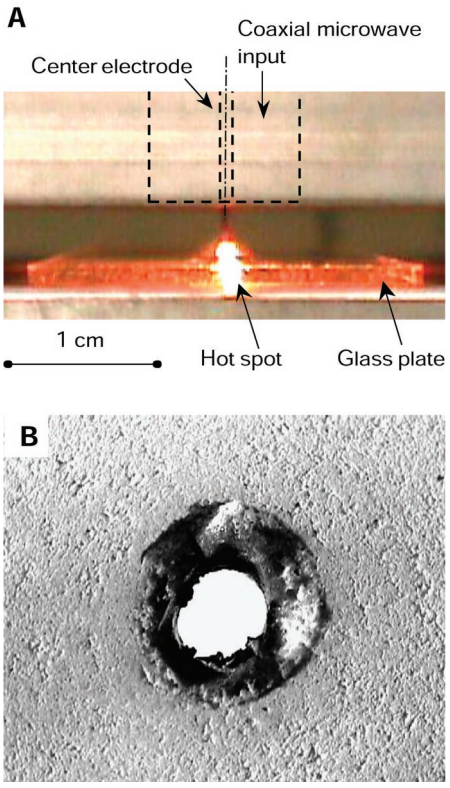

Fig. 2. (**A**) A hot spot created by a 1-mm-diameter microwave drill in a glass plate, as viewed from a side window of the applicator. The hidden coaxial feed is shown in broken lines. (**B**) An example of a microwave-drilled hole in low-purity alumina. The molten debris was not removed from the bore perimeter in order to show the effect.

Faculty of Engineering, Tel Aviv University, Ramat Aviv 69978, Israel.

*To whom correspondence should be addressed. E-mail: jerby@eng.tau.ac.il

The debris produced by the microwave drill was observed in three different forms: (i) compression of the solid material to the wall (in porous materials), (ii) evaporation and gas emission, and (iii) conversion to a glass solidified inside or outside the hole. Examples of (iii) are presented in Fig. 3, A and B, for concrete and ceramic, respectively. The glass formation inside a 2-cm-deep hole in a concrete brick (Fig. 3A) was caused by excessive microwave radiation after the drill was inserted. In Fig. 3B, the outflow of the glossy debris formed a crater outside the 1-mm-diameter hole made by drilling in a glass ceramic.

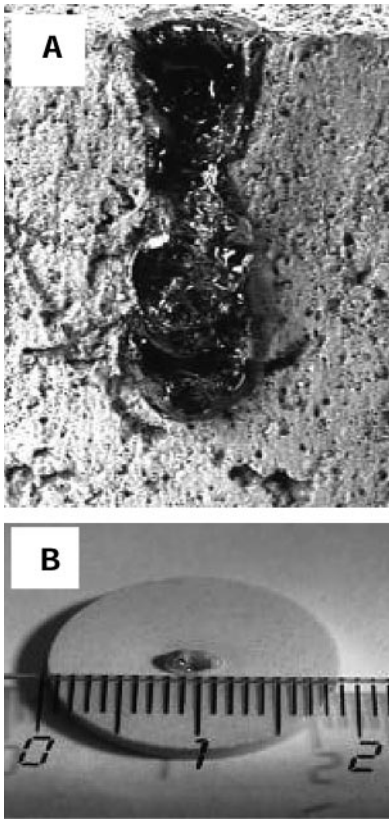

Fig. 3. (**A**) Glossy debris along a 2-cm-deep hole in a concrete brick caused by a further microwave radiation after the drill insertion. (**B**) A crater created by the debris outflow outside a 1-mm-diameter hole made in a glass ceramic.

The theoretical model of the microwave-drill operation couples the Maxwell and heat equations (*9*). It takes into account the temperature dependence of the material properties and effects of blackbody radiation and heat convection. A numerical simulation of the microwave-drill operation was developed using a finite-difference time-domain method (*10*). This simulation is simplified by a two–time-scale approach, because the electromagnetic-wave propagation is much faster than the thermal evolution. The simulation calculates the temperature evolution in front of the microwave drill. When the melting temperature is exceeded, it mimics the drill insertion into the material and updates the simulated geometry accordingly.

The temporal and spatial temperature evolution in front of the microwave drill was simulated for various materials. Figure 4A shows the resulting rapid temperature increase in front of the microwave drill (a coaxial feed with 1- and 10-mm inner and outer diameters, respectively; 137-ohm characteristic impedance; and 4-mm inner-rod insertion depth into the drilled material) for vitreous pottery clay. The temporal evolution of the temperature profile in front of the concentrator pin during the microwave illumination shows an increase in the temperature growth-rate above ~600°C, which resembles the thermal-runaway effect. Figure 4B shows the spatial distribution of the temperature around the inserted inner electrode, and the tight hot spot confinement for 200-W input radiation power. The electric-field component of the electromagnetic wave near the tip in Fig. 4B reaches a value of $\sim 1.5 \times 10^5$ V/m (peak).

A simplified analysis based on an open-end coaxial antenna model (*11*) buried in a lossy (but uniform) dielectric material provides a simple benchmark for the microwave-drill experiments and simulations. In this approach, equivalent lumped circuit elements such as a capacitor and a resistor model the effects of energy storage and power absorption, respectively, near the monopole antenna. This analysis defines the resonance conditions in which the impedance of the monopole antenna is resistive. Near resonance, most of the radiated microwave power is absorbed within a small volume around the antenna. The extended model provides estimates for the antenna impedance, its temperature dependence, the depth limitation ($<1/4$ wavelength) of the microwave-drill insertion, and the microwave power required for reaching melting in a given material and hole diameter.

Our study shows that the microwave drill is effective in the operating conditions presented above for dielectric materials characterized by dielectric losses and thermal conductivity in the ranges of $\varepsilon''/\varepsilon' \geq 0.003$ and $k_t \leq 10$ W/mK, respectively, where ε' and ε'' compose the complex dielectric constant, $\varepsilon = \varepsilon' - j\varepsilon''$. The material melting temperature should be lower

Table 1. A comparison of mechanical, laser-based, and microwave drills.

	Mechanical drills	Laser-based drills	Microwave drills
Main effect	Grinding by mechanical friction	Evaporation by infrared radiation	Melting (softening) by microwave heating
Mechanical contact	Yes	No	Yes
Mechanical motion	Fast rotation	No	Insertion, slow rotation
Radiation	No	Far-field (beam shape)	Near-field (localized)
Wavelength	–	Short ($\sim 10^{-5}$ m)	Long ($\sim 10^{-1}$ m)
Pollution	Dust, noise	Vapors	Microwave radiation
Diameter (typical)	10^3–10^0 m	10^{-6}–10^{-3} m	10^{-3}–10^{-2} m
Cost	Low	High	Medium

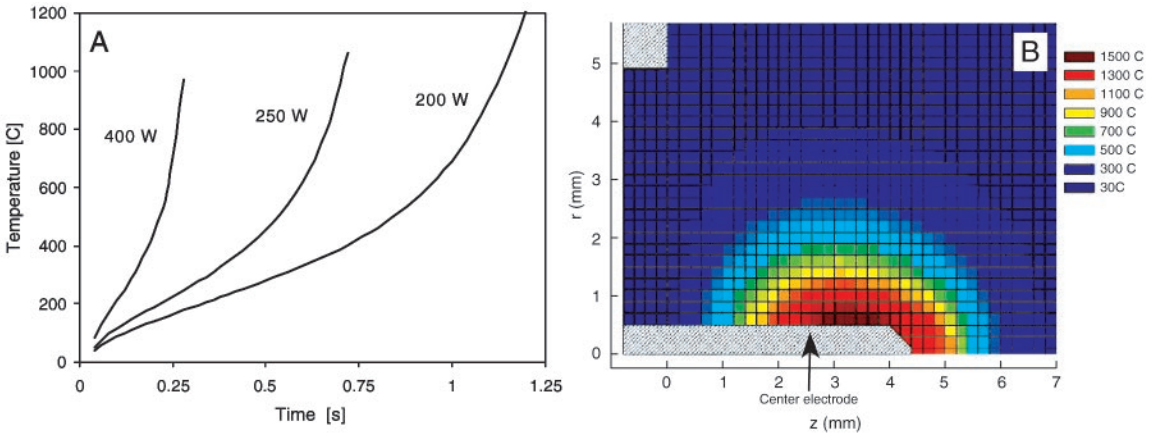

Fig. 4. Numerical simulations of the temperature evolution in front of the microwave drill (1- and 10-mm inner and outer diameters, respectively; 4-mm inner-rod insertion depth) in vitreous pottery clay. (**A**) Temporal rise at the peak point for different microwave power inputs. (**B**) Spatial distribution around the inserted drilling bit at 200-W microwave-power input.

than 2000°C (thus, for instance, the microwave drill has failed to penetrate into sapphire). To accelerate the thermal-runaway process, the material properties should be dependent on temperature in a way that the dielectric loss increases and/or the thermal conductivity decreases with increasing temperature. A positive temperature dependence of the dielectric losses characterizes many nonconductive materials (*12–14*). This feature increases the microwave power absorption in the evolved hot spot and therefore accelerates the temperature growth-rate and the thermal-runaway process. A preheating of such materials may also assist the microwave-drill operation.

Owing to thermal stresses, the microwave-drill operation on brittle materials such as silicon and glass may cause cracks (these were observed by optical and scanning-electron microscopes in ranges of 1 to 2 mm around some of the holes). This problem could be alleviated by a more gradual operation or by preheating. For larger holes, the affected zone could be removed mechanically during the microwave-drilling process. It should be noted, however, that in ceramics and aggregated materials the microwave drill may add a local sintering-like effect, and thus the material forming the walls may be strengthened.

Safety considerations impose certain limitations on the microwave drill operation, such as shielding to comply with safety standards. This could be implemented either by using a closed chamber (such as the domestic oven) or an open shielding plate (as illustrated in Fig. 1). The closed structure is applicable for automatic production lines, whereas the open shield may fit in construction and geological works. Both solutions were tested and resulted in <1 mW/cm^2 microwave power-density leakage, in accordance with common safety standards.

A comparison of the microwave-drill concept to mature drilling technologies is shown in Table 1 for mechanical and laser-based drills. The microwave drill integrates electromagnetic-radiation, heating, and mechanical effects, and in this sense it can be regarded as a hybrid method. However, unlike mechanical drills, the microwave-drill operation is quiet and clean. It does not contain fast rotating parts, nor does it cause mechanical friction, and its operation is essentially dust-free. On the other hand, the microwave drill emits hazardous radiation, which requires safety measures and limits its operating conditions.

The microwave-drill concept is not expected to compete with laser-based drills in accurate industrial tasks, but it should provide a low-cost solution for a variety of needs for holes in the millimeter-to-centimeter diameter range in common materials such as concrete, rocks, ceramics, silicates, and glasses. The microwave drill may find applications in industrial production lines, professional drilling-tools, and construction and geological equipment. It may also be most effective in low-cost applications that require silent, clean, and efficient operation.

References and Notes

1. K. Krajick, *Science* **283**, 781 (1999).
2. J. F. Ready, *Industrial Applications of Lasers* (Academic Press, New York, 1997).
3. J. Thuery, *Microwave: Industrial, Scientific, and Medical Applications* (Artech House, Boston, 1992).
4. D. P. Lindroth, R. J. Morrell, J. R. Blair, U.S. Patent 5,003,144 (1991).
5. A. C. Metaxas, *Foundations of Electroheat—A Unified Approach* (Wiley, Chichester, UK, 1996).
6. P. E. Parris, V. M. Kenkre, *Phys. Status Solidi* (*b*) *Basic Res.* **200**, 39 (1997).
7. C. A. Vriezinga, *J. Appl. Phys.* **83**, 438 (1998).
8. E. Jerby, V. Dikhtyar, U.S. Patent 6,114,676 (2000).
9. U. Grosglick, V. Dikhtyar, E. Jerby, paper presented at the European Symposium on Numerical Methods in Electromagnetics, (JEE'02), Toulouse, France, 6 to 8 March 2002.
10. Y. Alpert, E. Jerby, *IEEE Trans. Plasma Sci.* **27**, 555 (1999).
11. R. W. P. King, C. W. Harrison, *Antennas and Waves: A Modern Approach* (MIT Press, Cambridge, MA, 1969).
12. N. G. Evans, M. G. Hamlyn, *Mater. Res. Soc. Symp. Proc.* **430**, 9 (1996).
13. R. M. Hutcheon *et al.*, *Mater. Res. Soc. Symp. Proc.* **269**, 541 (1992).
14. A. Birnboim *et al.*, *J. Am. Ceram. Soc.* **81**, 1493 (1998).

15. We acknowledge the support of the State-of-Israel Ministry of National Infrastructures, the Belfer Foundation, and the Schechterman Foundation.

24 April 2002; accepted 11 September 2002

Kilimanjaro Ice Core Records: Evidence of Holocene Climate Change in Tropical Africa

Lonnie G. Thompson,[1,2]* Ellen Mosley-Thompson,[1,3] Mary E. Davis,[1,2] Keith A. Henderson,[1,2] Henry H. Brecher,[1] Victor S. Zagorodnov,[1,2] Tracy A. Mashiotta,[1] Ping-Nan Lin,[1] Vladimir N. Mikhalenko,[4] Douglas R. Hardy,[5] Jürg Beer[6]

Six ice cores from Kilimanjaro provide an ~11.7-thousand-year record of Holocene climate and environmental variability for eastern equatorial Africa, including three periods of abrupt climate change: ~8.3, ~5.2, and ~4 thousand years ago (ka). The latter is coincident with the "First Dark Age," the period of the greatest historically recorded drought in tropical Africa. Variable deposition of F^- and Na^+ during the African Humid Period suggests rapidly fluctuating lake levels between ~11.7 and 4 ka. Over the 20th century, the areal extent of Kilimanjaro's ice fields has decreased ~80%, and if current climatological conditions persist, the remaining ice fields are likely to disappear between 2015 and 2020.

Few continuous, high-temporal-resolution climate histories are available from the tropics, although climate variability in this region strongly forces the global climate system. A modest number of ice core records exist for South America, the Himalayas, and the Tibetan Plateau, and here we present the first ice core–based climate history for Africa, recovered from the ice fields atop Kilimanjaro. In January and February of 2000, six ice cores (Fig. 1) were drilled to bedrock on three remnant ice fields on the rim and summit plateau of Kilimanjaro (3°04.6′S; 37°21.2′E; 5893 m above sea level). These cores provide the last opportunity to establish an ice core record of African climate. The three longest cores (NIF1, NIF2, and NIF3) were drilled to depths of 50.9, 50.8, and 49.0 m, respectively, from the Northern Ice Field (NIF), the largest of the ice bodies. Two shorter cores (SIF1 and SIF2) were drilled to bedrock on the Southern Ice Field (SIF) to depths of 18.5 and 22.3 m, respectively, and a 9.5-m core was drilled to bedrock on the small, thin Furtwängler Glacier (FWG) within the crater. Temperatures were measured in each borehole; in the NIF, they ranged from –1.2°C at 10 m depth to –0.4°C at bedrock, and in the SIF, they were near 0°C. No evidence of water was observed in the boreholes on the NIF or SIF, but the FWG was water-saturated throughout. Sampling and analysis details are provided in the supporting online text.

Aerial photographs taken on 16 February 2000 allowed production of a recent detailed map of ice cover extent on the summit plateau (Fig. 1). Concurrent with the drilling program,

[1]Byrd Polar Research Center, [2]Department of Geological Sciences, [3]Department of Geography, The Ohio State University, Columbus, OH 43210, USA. [4]Institute of Geography, Moscow, Russia. [5]Department of Geosciences, University of Massachusetts, Amherst, MA 01003–9297, USA. [6]Swiss Federal Institute for Environmental Science and Technology (EAWAG) Duebendorf, Switzerland.

*To whom correspondence should be addressed. E-mail: thompson.3@osu.edu